Reciprocal regulation of glycine-rich RNA-binding proteins via an interlocked feedback loop coupling alternative splicing to nonsense-mediated decay in Arabidopsis

Jan C. Schöning[1], Corinna Streitner[1], Irmtraud M. Meyer[2,3], Yahong Gao[1] and Dorothee Staiger[1,*]

[1]Molecular Cell Physiology, Bielefeld University, Bielefeld, Germany, [2]UBC Bioinformatics Centre, Department of Computer Science and [3]Department of Medical Genetics, University of British Columbia, Vancouver, BC, Canada

ABSTRACT

The Arabidopsis RNA-binding protein *At*GRP8 undergoes negative autoregulation at the post-transcriptional level. An elevated *At*GRP8 protein level promotes the use of a cryptic 5′ splice site to generate an alternatively spliced transcript, as_*AtGRP8*, retaining the 5′ half of the intron with a premature termination codon. In mutants defective in nonsense-mediated decay (NMD) abundance of as_*AtGRP8* but not its pre-mRNA is elevated, indicating that as_*AtGRP8* is a direct NMD target, thus limiting the production of functional *At*GRP8 protein. In addition to its own pre-mRNA, *At*GRP8 negatively regulates the *AtGRP7* transcript through promoting the formation of the equivalent alternatively spliced as_*AtGRP7* transcript, leading to a decrease in *At*GRP7 abundance. Recombinant *At*GRP8 binds to its own and the *AtGRP7* pre-mRNA, suggesting that this interaction is relevant for the splicing decision *in vivo*. *At*GRP7 itself is part of a negative autoregulatory circuit that influences circadian oscillations of its own and the *AtGRP8* transcript through alternative splicing linked to NMD. Thus, we identify an interlocked feedback loop through which two RNA-binding proteins autoregulate and reciprocally crossregulate by coupling unproductive splicing to NMD. A high degree of evolutionary sequence conservation in the introns retained in as_*AtGRP8* or as_*AtGRP7* points to an important function of these sequences.

INTRODUCTION

Post-transcriptional regulation has come into focus as an important mechanism to control gene expression in higher plants (1–4). It occurs at multiple levels including pre-mRNA maturation, mRNA transport, translation and breakdown. The major players are RNA-binding proteins that influence the fate of an mRNA molecule either directly by binding to defined RNA sequences and structural elements or indirectly through protein–protein interaction (5).

One important protein domain known to interact with RNA molecules is the RNA recognition motif (RRM) (6). It is composed of a four-stranded antiparallel β-sheet with two α-helices. The highly conserved octapeptide RNP1 and hexapeptide RNP2 sequence motifs are located in the β_3 and β_1 sheets and contain conserved aromatic residues making contacts to the RNA substrate. A systematic survey disclosed 196 RRM-containing proteins in the genome of *Arabidopsis thaliana* (5). Among those, the 16 kDa *At*GRP8 (*A. thaliana* glycine-rich RNA-binding protein 8) protein combines a single N-terminal RRM with a C-terminal region enriched in glycine repeats with some interspersed serine, tyrosine and arginine residues (7–9). It is also known as GR-RBP8, GRP8 or CCR1 (cold and circadian regulated 1) (5,10,11). Both *AtGRP8* and *AtGRP7* encoding an orthologous RNA-binding protein that shares 77% sequence identity undergo circadian oscillations with a peak at the end of the daily light phase (9,11). Notably, *At*GRP8 is subject to negative regulation by *At*GRP7, as in transgenic plants ectopically overexpressing *At*GRP7 under control of the CaMV (Cauliflower Mosaic Virus) 35S RNA promoter,

---

*To whom correspondence should be addressed. Tel: +49 521 106 5609; Fax: +49 521 106 6410; Email: dorothee.staiger@uni-bielefeld.de

AtGRP8 oscillations are strongly depressed (9). This regulation occurs at the post-transcriptional level through reduction of constitutive splicing and stimulation of alternative splicing at a cryptic intronic 5′ splice site of the *AtGRP8* pre-mRNA, leading to an alternative splice variant (as_*AtGRP8*) with a premature termination codon (PTC) in the retained part of the intron.

*At*GRP7 uses the same mechanism for negative autoregulation: rising protein levels promote alternative splicing by binding to its own pre-mRNA, and the alternatively spliced transcript (as_*AtGRP7*) is degraded via a pathway involving the nonsense-mediated decay (NMD) components AtUPF1 (UP FRAMESHIFT PROTEIN 1) and AtUPF3 (12,13). Thus, *At*GRP7 is part of a negative feedback loop through which it influences its own oscillation at the post-transcriptional level. This feedback loop is thought to operate as a slave oscillator downstream of the circadian clock, transducing temporal information within the cell by regulating other transcripts (13,14).

We have recently found that *At*GRP8 acts in concert with *At*GRP7 to influence the transition to flowering in *A. thaliana* (15). Apart from this, little is known about *At*GRP8 function within the cell.

Here we show that *At*GRP8 forms a feedback loop that is interlocked with the *At*GRP7 feedback loop. Recombinant *At*GRP8 interacts with its own mRNA *in vitro* and promotes negative autoregulation *in vivo* by causing alternative splicing. The parts of the intron that are retained in the unproductively spliced transcripts show an exon-like evolutionary conservation, pointing to a functional role. As the alternatively spliced *AtGRP8* and *AtGRP7* transcripts are *bona fide* NMD targets, it appears that the interlocked *At*GRP7/*At*GRP8 feedback loops harness autogenous alternative splicing-activated decay via the NMD pathway to fine-tune the expression of their components.

MATERIALS AND METHODS

*At*GRP8 overexpression in transgenic plants

The protein-coding region of *AtGRP8* was amplified by PCR from the cDNA with the upstream primer 5′ GG<u>CCATGG</u>CTGAAGTTGAGT 3′ and the downstream primer 5′ CC<u>GGATCC</u>TT**TA**CCAGCCGCCAC CAC 3′ covering the translation start and stop (bold) and comprising engineered NcoI and BamHI sites (underlined), respectively. The PCR product was inserted between the CaMV 35S RNA promoter with the duplicated enhancer fused to the Tobacco Mosaic Virus omega translational enhancer and the CaMV polyadenylation signal (9). To express *AtGRP8*-RQ, the Arg[47]Gln mutation was introduced by PCR-mutagenesis (see below), sequenced and reinserted into the original plasmid by BglII/SacI digestion. The entire casettes were inserted into the binary vector **pHPT1** that was obtained by replacing the promoter-less β-glucuronidase gene of pGPTV-HPT by the pUC19 polylinker (16). *Arabidopsis thaliana* L. Columbia plants were transformed by vacuum infiltration (17).

Plant growth

Seeds were germinated on one-half strength MS plates (18) containing 0.5% sucrose and the appropriate antibiotic and grown in 16 h light/8 h dark cycles at a constant temperature of 20°C. After 2 weeks, resistant plants were transferred to one-half strength MS plates without antibiotics.

Recombinant GST-*At*GRP8 and GST-*At*GRP8-RQ

Recombinant GST-*At*GRP8 protein was constructed by inserting the *AtGRP8* coding region into NotI-EcoRI-cut **pGEX-6P1** vector (GE Healthcare, Freiburg, Germany).

To generate the mutant variant GST-*At*GRP8-RQ, Arg[47] in GST-*At*GRP8 was exchanged for glutamine by PCR with Phusion Polymerase (Finnzymes, Espoo, Finland) using the overlapping primers RQ$_{for}$ CGA GAGTGGAAGATC<u>CCAAGGAT</u>-TCGGATTCGTCA and RQ$_{rev}$ TGACGAATCCGAATC<u>CTTGGGAT</u>CTT CCACTCTCG. Silent mutations were introduced into neighbouring amino acids creating a diagnostic *Sty*I site (underlined). The mutation was verified by sequencing. The recombinant proteins were expressed in *E. coli* BL21 DE3. Affinity purification by chromatography on Glutathione Sepharose (GE Healthcare) and concentration of the eluate by centrifugation through Centricon® 30 filter devices (Millipore, Billerica, MA, USA) were done as described (12,13).

RNA-binding assay

Synthetic oligoribonucleotides (ORN) were purchased from Biomers (Ulm, Germany). RNA bandshifts with recombinant *At*GRP8 and the ORNs labelled at the 5′ end with γ-[^{32}P] ATP were performed as previously described (12). To determine binding affinities, 50 fmol of labeled ORN-binding substrates were incubated with increasing amounts of recombinant protein, respectively, in the presence of 1 μg tRNA. Bound and free RNA were quantified and K_d values calculated based on three independent experiments as described (12).

RNA analysis

Isolation of total RNA from Arabidopsis plants and hybridization of RNA gel blots with the gene-specific *AtGRP7* and *AtGRP8* probes were performed as described (8,19). Semiquantitative RT–PCR on retrotranscribed total RNA was done as described (15). Primers are listed in Table S2.

Immunoblot analysis

Protein extraction from Arabidopsis plants and incubation of protein gel blots with antipeptide antibodies raised against *At*GRP8 and *At*GRP7, followed by chemiluminescence detection were done as described (12).

Secondary structure prediction

Evolutionary conserved RNA secondary structure elements were determined with the RNA-Decoder program (20,21). RNA-Decoder takes as input a fixed alignment

of evolutionarily related RNA sequences and an evolutionary tree relating them and predicts as output the conserved secondary structures supported by the evolutionary patterns detected in the input alignment. A set of nine pre-mRNA sequences comprising *AtGRP8* orthologs with the same gene structure comprising a 5′ UTR, two protein-coding exons of phase 0, a single intron and a 3′ UTR (Table S1) were assembled. To generate the input alignment, we first compiled separate alignments for 5′ UTRs, exon 1, intron, exon 2 and 3′ UTRs using ClustalW (Version 1.83) (22), which we then combined manually into longer alignments. To maximize the alignment quality, the alignments of the pre-mRNA sequences of exons 1 and 2 were based on the ClustalW alignments of the corresponding encoded amino-acid sequences. As the resulting full-length pre-mRNA alignment (1407 nt) was too long to analyze in a single chunk, we generated an mRNA input alignment with UTRs (1055 nt) to investigate conserved secondary structures in or near the UTRs and a pre-mRNA input alignment without UTRs (1093 nt) to investigate conserved secondary structures in or near the intron.

RESULTS AND DISCUSSION

*At*GRP8 negatively autoregulates its own pre-mRNA

To begin to investigate the molecular properties of the predicted RNA-binding protein *At*GRP8, we generated transgenic plants ectopically overexpressing the *AtGRP8* coding region under control of the CaMV promoter with the duplicated enhancer (*AtGRP8*-ox plants). Immunoblot analysis using a specific *At*GRP8 antibody identified transgenic lines with strongly elevated *At*GRP8 protein levels (Figure 1A). Compared to WT plants, the total *AtGRP8* transcript level was strongly elevated in *At*GRP8-ox plants harvested at zt3 (zeitgeber time 3, that is 3 h after lights on), the circadian minimum of *AtGRP8* oscillations, and zt11, the circadian maximum, due to the expression of the transgene (Figure 1C). The endogenous *AtGRP8* transcript forms are selectively detected with a gene-specific probe derived from the 5′ UTR that is not contained in the overexpression construct (Figure 1C). In WT plants, the endogenous *AtGRP8* mRNA and a small amount of its pre-mRNA containing the 283-nt intron were present. In the *AtGRP8*-ox plants, almost no mature endogenous *AtGRP8* mRNA was detectable. Instead, an intermediate size transcript appears at a low level, corresponding to the alternatively spliced *AtGRP8* transcript (as_*AtGRP8*) that is generated through the use of a cryptic 5′ splice site within the intron. These data indicate that *AtGRP8* exerts negative autoregulation on its own pre-mRNA.

In WT plants, as_*AtGRP8* is hardly detectable. Nevertheless, corresponding cDNAs have been isolated from cDNA libraries (DS, unpublished results). In response to the elevated *At*GRP8 protein level, a shift to a cryptic 5′ splice site occurs and as_*AtGRP8* accumulates to a low level at the expense of the mature mRNA in *At*GRP8-ox plants. Because the retained part of the intron contains in-frame stop codons, no full-length
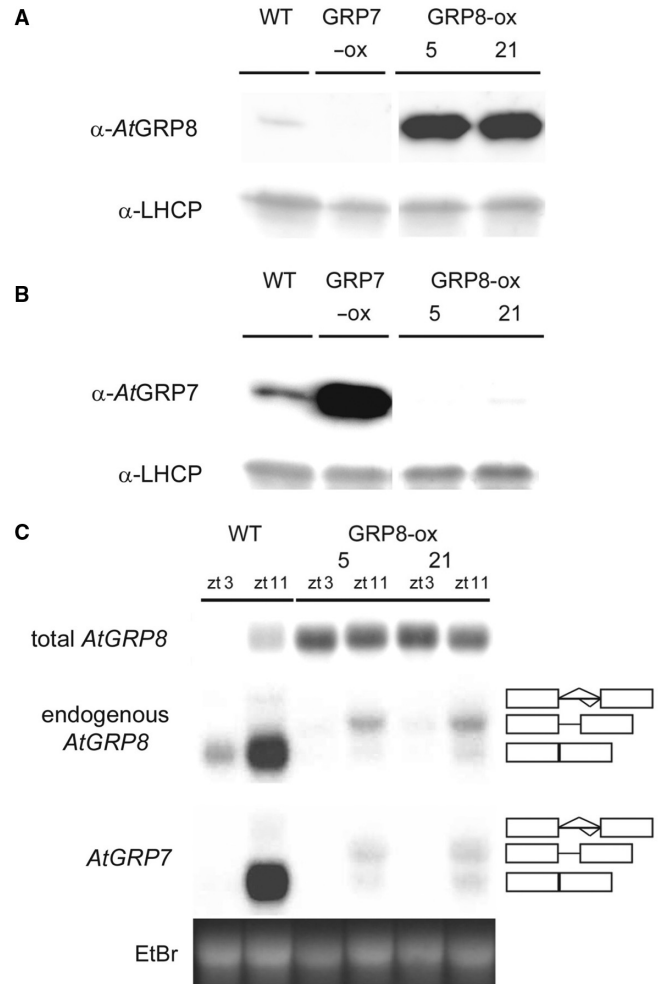

Figure 1. Influence of ectopic *At*GRP8 overexpression on the endogenous *AtGRP7* and *AtGRP8*. (**A**) The immunoblot with total protein of WT plants, the *At*GRP8-ox lines 5 and 21 and an *At*GRP7-ox line, harvested at zt11, was probed with the *At*GRP8 antibody (top) and an antibody against LHCP (light harvesting chlorophyll-binding protein) as loading control (bottom). The absence of crossreaction with overexpressed *At*GRP7 protein in *At*GRP7-ox plants demonstrates the specificity of the antibody. (**B**) A duplicate blot was probed with the *At*GRP7 antibody (top) and the LHCP antibody (bottom). (**C**) WT and *At*GRP8-ox plants were harvested at zt3 and zt11. The RNA gel blot was hybridized with the *AtGRP8* cDNA to determine the total *AtGRP8* transcript level. The stripped blot was rehybridized with the gene-specific probe to monitor the endogenous *AtGRP8* transcript and subsequently with the gene-specific *AtGRP7* probe. The position of the pre-mRNA, as_*AtGRP8* and as_*AtGRP7* retaining the first half of the intron and the mature mRNA are indicated. Boxes represent exons, lines represent the first and second half of the intron, respectively. The ethidium-bromide stained gel shows equal loading.

*At*GRP8 protein can be produced from the as_*AtGRP8* transcript. Thus, like *At*GRP7, *At*GRP8 negatively autoregulates, and the molecular underpinnings of the *At*GRP8 feedback loop are similar to the way *At*GRP7 influences its own circadian oscillations (12,13).

*At*GRP8 promotes alternative splicing of the *AtGRP7* pre-mRNA

To test whether *At*GRP8 would also influence *AtGRP7* transcript abundance, the *AtGRP7* transcript level was

Table 1. Sequences of oligoribonucloetides used as RNA-binding substrates

Name	Sequence
8-UTR_WT	GUUUUUGGUUUAGAUUUGGUUUUGUGU
8-UTR_G$_6$mut	GUUUUU**A**AUUU**A**A**A**UUU**A**AUUUU**A**UGU
8-UTR_938	CGUUUGGUUUACUUUUUUGAUGAAACA
8-intron_WT	CUUCCACGAUUGUUUUUGCUGAUGUGU
8-intron_G$_2$U$_2$mut	CUUCCACGAUU**A**U**CC**UU**A**CUGAUGUGU
7-UTR_WT	AUUUUGUUCUGGUUCUGCUUUAGAUUUGAUCU
7-UTR_G$_4$mut	AUUUU**A**UUCU**A**AUUCUGCUUU**A**GAUUU**A**AUCU
7-intron_WT	GUUCAGUUUUGUUGGAUUGUUUUGCUGAUCUG
7-intron_G$_6$mut	GUUC**A**AUUUU**A**UU**A**A**A**UU**A**UUUU**A**CUGAUCUG

Sequences of the *AtGRP8* 3′ UTR (8-UTR_WT and 8-UTR_938) and intron (8-intron_WT) ORN and the corresponding mutated 8-UTR_G$_6$mut and 8-intron_G$_2$U$_2$mut with six G residues exchanged for A or two G and two U residues exchanged for A or C (in bold), respectively, as well as sequence of *AtGRP7* 3′ UTR (7-UTR_WT) and intron (7-intron_WT) ORN and the corresponding mutated 7-UTR_G$_4$mut and 7-intron_G$_6$mut with four or six G residues exchanged for A (in bold), respectively, are shown.

compared in WT and *At*GRP8-ox plants (Figure 1C). In WT plants, the mature *AtGRP7* mRNA and a small amount of the pre-mRNA were detected at the circadian maximum. When *At*GRP8 was expressed at high levels, a low amount of the as_*AtGRP7* transcript appeared at the expense of the mature mRNA. Accordingly, *At*GRP7 protein was barely detectable in the *At*GRP8-ox plants (Figure 1B).

AtGRP8 RNA and protein steady-state abundance previously have been shown to be under negative control by *At*GRP7 (12,13). Consistent with this, *AtGRP8* RNA and protein levels are elevated in the *atgrp7-1* T-DNA insertion mutant due to relief of repression (15). Our data now show that not only does *At*GRP7 influence *AtGRP8* abundance, but also *At*GRP8 in turn regulates *AtGRP7*. Similarly, another Arabidopsis splicing regulator, the Ser/Arg-rich (SR) protein atRSZ33 crossregulates alternative splicing of a conserved long intron in the atRSp31 gene, equivalent to the effect on its own pre-mRNA (23,24). The alternative atRSp31 form accumulates to high levels and thus is stable in contrast to as_*AtGRP8*.

Recombinant *At*GRP8 binds to its own pre-mRNA

As *AtGRP7* autoregulation involves *At*GRP7 binding to its own 3′ UTR and intron, it is conceivable that *At*GRP8 might similarly interact with its own pre-mRNA. Therefore, we performed RNA-bandshift assays to test the *At*GRP7-binding sites determined previously (12) for interaction with recombinant *At*GRP8 (Table 1). For the intronic binding site 8-intron_WT GST-*At*GRP8 formed a retarded complex which was competed more efficiently by the ORN 8-intron_WT than by the mutated counterpart 8-intron_G$_2$U$_2$mut with exchanges of two G and two U residues (Figure 2A). For the 3′ UTR, a retarded complex was observed for 8-UTR_WT that was more efficiently outcompeted by unlabeled ORN 8-UTR_WT than by the mutated counterpart 8-UTR_G$_6$mut with mutation of six G residues (Figure 2B). Sequence alignment of the *At*GRP7-binding sites upon the *AtGRP8*

intron and 3′ UTR had uncovered a second motif with homology to the *At*GRP7-binding site within the *AtGRP8* 3′ UTR (data not shown). However, determination of the K_d values revealed that *At*GRP8 has a 10-fold lower affinity for the corresponding ORN 8-UTR_938 (Table 1) compared to 8-UTR_WT (Figure 2C). Furthermore, the complex was outcompeted by an excess of unlabeled 8-UTR_938 to the same degree as by a negative control ORN 7-UTR_G$_4$mut (Table 1) (Figure 2D). Based on the low affinity and lack of specificity, 8-UTR_938 was excluded as binding site. Taken together, our data show that *At*GRP8 binds to its own pre-mRNA and recognizes sequences in the second half of the intron and the 3′ UTR that also comprise targets for *At*GRP7.

To assess the secondary structure of these putative binding sites in the context of the entire pre-mRNA, *At*GRP8 was searched for secondary structure elements conserved in plant orthologs with RNA-Decoder (20,21). Among the numerous existing secondary structure prediction programs, RNA-Decoder is unique in that it explicitly takes the known protein-coding regions of an input alignment into account. This feature is important when searching partly protein-coding sequences such as pre-mRNAs for conserved secondary structure elements, as the evolutionary pattern due to amino-acid conservation needs to be carefully distinguished from the evolutionary pattern due to secondary structure conservation (20,21).

In order to detect conserved secondary structures in the *AtGRP8* pre-mRNA, we assembled a set of nine pre-mRNA sequences comprising *AtGRP8* as well as eight *AtGRP8* orthologs from the *Brassicaceae* mustard and oilseed rape, the other dicotyledoneous plants tobacco and Pelargonium, and the monocotyledoneous plants rice and maize (Table S1). As input tree to RNA-Decoder, we used the tree predicted by ClustalW (22) for the nine encoded protein sequences. The predicted secondary structures for the *AtGRP8* and, for comparison, the *AtGRP7* pre-mRNAs are shown in Figure S1. Interestingly, the predicted *At*GRP8-binding sequences map to conserved regions, pointing to an important role of the secondary structure for the function of these motifs. 8-intron_WT and 8-UTR_WT are predicted to be single-stranded. In contrast, 8-UTR_938 is predicted to be partially double-stranded and thus may be less accessible to interacting proteins, in line with the very low binding affinity (Figure 2C).

Recombinant *At*GRP8 binds to the *AtGRP7* pre-mRNA

The data shown in Figure 1 indicate that *At*GRP8 negatively influences *AtGRP7* pre-mRNA splicing in the same way as *At*GRP7 autoregulates. As the shift to the alternative splice form relies on *At*GRP7 binding to its own pre-mRNA, we tested whether recombinant *At*GRP8 would bind *in vitro* to the *At*GRP7 target sites within the *AtGRP7* pre-mRNA (Table 1). Complex formation was observed with 7-UTR_WT that was completely lost upon addition of 250 pmol of unlabeled 7-UTR_WT, but much less reduced with 500 pmol of the mutated 7-UTR_G$_4$mut (Figure 3A). Also for the ORN spanning the *At*GRP7-binding site within the second half of the
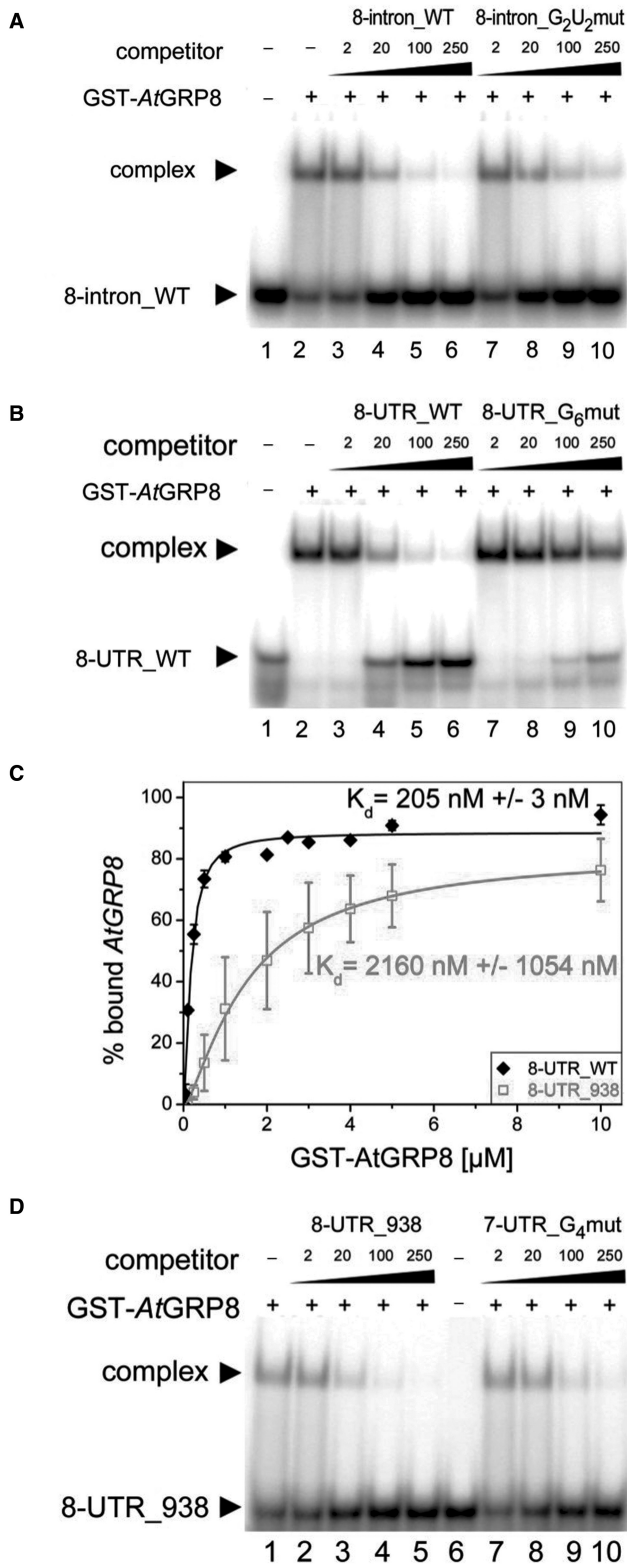
Figure 2. Binding of recombinant *At*GRP8 to the *AtGRP8* transcript. (**A**) GST-*At*GRP8 protein was incubated with labelled 8-intron_WT ORN in the presence of 5 µg of tRNA and 2, 20, 100 and 250 pmol of unlabelled 8-intron_WT ORN (lanes 3–6) or 8-intron_G_2U_2mut (lanes 7-10), respectively. Lane 1, free ORN. (**B**) GST-*At*GRP8 protein was incubated with labelled 8-UTR_WT ORN in the presence of 5 µg of tRNA and 2, 20, 100 and 250 pmol of unlabelled 8-UTR_WT ORN (lanes 3–6) or 8-UTR_G_6mut (lanes 7-10), respectively. Lane 1, free ORN. (**C**) To compare binding affinities, 50 fmol of labelled 8-UTR_WT ORN or 8-UTR_938 were incubated with 0.01, 0.05, 0.1, 0.25, 0.5, 1, 2, 2.5, 5 and 10 µM or 0.1, 0.25, 0.5, 1, 2, 3, 4, 5 and 10 µM of GST-*At*GRP8, respectively. All reactions contained 1 µg tRNA. Bound and free RNA were quantified and K_d values calculated based on the mean of three independent experiments as described (12). (**D**) GST-*At*GRP8 protein was incubated with labelled 8-UTR_938 ORN in the presence of 5 µg of tRNA and 2, 20, 100 and 250 pmol of unlabelled 8-UTR_938 ORN (lanes 2–5) or 7-UTR_ G_4mut (lanes 7–10), respectively. Lane 6, free ORN.

intron a strong interaction with GST-*At*GRP8 was found which was abolished by 250 pmol of unlabeled 7-intron_WT but not affected by 500 pmol of 7-intron G_6mut (Figure 3B). This shows that *At*GRP8 also binds to the *AtGRP7* intron and 3′ UTR with a certain specificity. Thus, *AtGRP7* and *AtGRP8* may recognize overlapping or identical motifs within both pre-mRNAs. To compare the binding affinities, K_d values were determined for all interactions (Table 2). For the four binding sites, the K_d values were in the same order of magnitude as those previously determined for GST-*At*GRP7 protein (12). Therefore, presently we cannot infer which of the possible interactions between *AtGRP7* or *AtGRP8* and the respective target sites may prevail *in vivo*.

Mutation of *At*GRP8 RNP1 Arg[47] impairs RNA-binding activity *in vitro*

Binding of *At*GRP8 to its own and the *AtGRP7* pre-mRNA *in vitro* suggests that this interaction may initiate alternative splicing and down-regulation of endogenous *AtGRP7* and *AtGRP8 in vivo*. To investigate whether this *in vitro* binding activity correlated with *in vivo* function, a mutation was introduced into the RRM of recombinant GST-*At*GRP8. The conserved arginine (R) 47 predicted to lie at the beginning of the β3 strand that is part of the RNA-binding platform was exchanged for glutamine (Q) (25–27). Indeed, we have shown that recombinant GST-*At*GRP7-RQ with an analogous mutation of R[49] has a 6-fold lower affinity for its target sites than WT GST-*At*GRP7 protein while folding of the protein is not affected (12).

The *At*GRP8-RQ mutant protein was expressed as GST-fusion and tested for binding to the *AtGRP7* and *AtGRP8* target sites. Only weak interaction was observed with K_d values about one order of magnitude higher for GST-*At*GRP8-RQ compared to GST-*At*GRP8 (Table 2). Competition assays revealed that 8-UTR_WT competed much better for binding of GST-*At*GRP8-RQ than 8-UTR_G_6mut and 7-UTR_WT competed much better for binding of GST-*At*GRP8-RQ than 7-UTR_G_4mut (data not shown). Thus, mutation of the conserved R[47] reduces the binding affinity rather than the specificity of the interaction.

The *At*GRP8 R[47]Q mutation impairs but does not abolish promotion of alternative *AtGRP8* and *AtGRP7* splicing

To test the impact of the RQ mutation on *At*GRP8 activity *in vivo*, plants constitutively overexpressing the mutated *At*GRP8-RQ protein were generated (*At*GRP8-RQ-ox) and compared to plants overexpressing WT *At*GRP8 protein (*At*GRP8-ox). Transgenic plants were
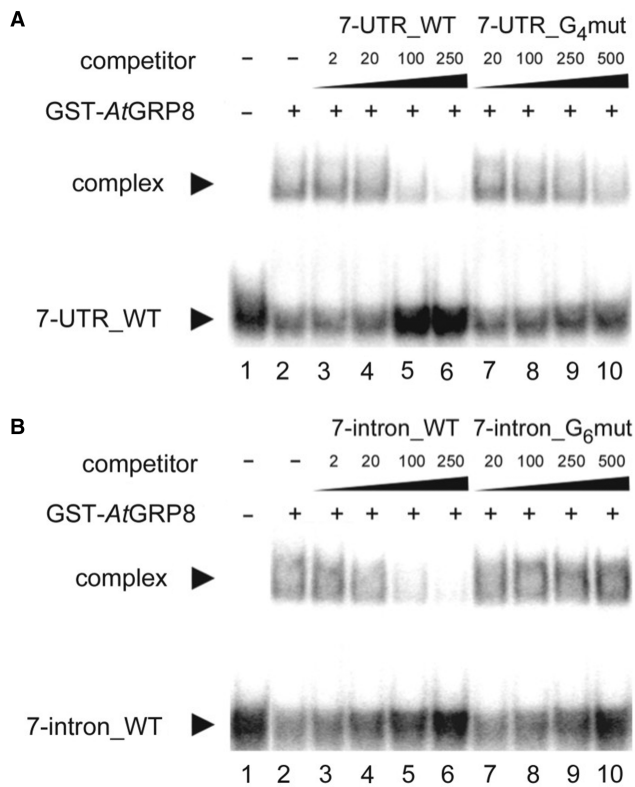
Figure 3. Binding of recombinant *AtGRP8* to the *AtGRP7* transcript. (**A**) GST-*AtGRP8* protein was incubated with labelled 7-UTR_WT ORN in the presence of 5 μg of tRNA and 2, 20, 100 and 250 pmol of unlabelled 7-UTR_WT ORN (lanes 3–6) or 20, 100, 250 and 500 pmol of unlabelled 7-UTR_G$_4$mut (lanes 7–10), respectively. Lane 1, free ORN. (**B**) GST-*AtGRP8* protein was incubated with labelled 7-intron_WT ORN in the presence of 5 μg of tRNA and 2, 20, 100 and 250 pmol of unlabelled 7-intron_WT ORN (lanes 3–6) or 20, 100, 250 and 500 pmol of unlabelled 7-intron_G$_6$mut ORN (lanes 7–10), respectively. Lane 1, free ORN.

Table 2. K_d values for recombinant GST-*At*GRP8-RQ and GST-*At*GRP8

ORN	Protein	K_d [M]	K_d RQ/K_d WT
8-UTR_WT	GST-*At*GRP8-WT	$2.05 \pm 0.03 \times 10^{-7}$	
	GST-*At*GRP8-RQ	$1.31 \pm 0.35 \times 10^{-6}$	6.4
7-UTR_WT	GST-*At*GRP8-WT	$3.18 \pm 2.27 \times 10^{-7}$	
	GST-*At*GRP8-RQ	$3.22 \pm 0.97 \times 10^{-6}$	10.1
8-intron_WT	GST-*At*GRP8-WT	$1.64 \pm 0.65 \times 10^{-6}$	
	GST-*At*GRP8-RQ	$2.29 \pm 0.36 \times 10^{-5}$	14.0
7-intron_WT	GST-*At*GRP8-WT	$4.26 \pm 0.52 \times 10^{-7}$	
	GST-*At*GRP8-RQ	$3.59 \pm 2.02 \times 10^{-6}$	8.4

K_d values were determined as described in (12). The ratio between the K_d value for the mutated protein and the WT protein is indicated.

identified with a total *AtGRP8* transcript level constitutively elevated at zt3 and zt11 (Figure 4A, top). An immunoblot analysis confirmed expression of intact mutated protein, as total *At*GRP8 protein was elevated to a level similar to that in *At*GRP8-ox plants overexpressing WT *At*GRP8 protein (Figure 4B). However, in contrast to *At*GRP8-ox plants, the mature endogenous *AtGRP8* mRNA was still detected in addition to as_*AtGRP8* (Figure 4A, middle). Thus, an elevated *At*GRP8-RQ level only partially shifts the splice site in favor of the cryptic 5′ splice site with concomitant reduction in as_*AtGRP8* abundance, as observed in *At*GRP8-ox plants. We infer from this that the weakened interaction of *At*GRP8-RQ with its own pre-mRNA impairs but does not abolish negative autoregulation of the *AtGRP8* pre-mRNA.

Overexpression of WT *AtGRP8* led to an accumulation of as_*AtGRP7* and an almost complete loss of the mature mRNA (Figure 4C). In contrast, no alternatively spliced *AtGRP7* transcript was detected in *At*GRP8-RQ-ox plants. Thus, the R^{47}Q mutation reduces the effect *At*GRP8 protein has on splice site selection. The level of mature *AtGRP7* mRNA was only weakly reduced compared to WT plants, consistent with the idea that the residual binding activity of *At*GRP8-RQ still causes some production of as_*AtGRP7* at the expense of the *AtGRP7* mRNA. However, the alternatively spliced transcript is hardly detectable due to its short half life (13). Accordingly, almost no *At*GRP7 protein was detected in *At*GRP8-ox plants, whereas a small amount of *At*GRP7 protein was detectable in *At*GRP8-RQ-ox lines (Figure 4D). Altogether, the interaction of *At*GRP8 with the *AtGRP7* and *AtGRP8* pre-mRNAs *in vivo* is relevant for the negative autoregulation and crossregulation. Presumably, binding of *At*GRP8 and *At*GRP7 triggers additional factors that act in concert to regulate the choice of splice sites (12).

Distinct cold response of *At*GRP8 and *At*GRP7

The reciprocal regulation between *At*GRP7 and *At*GRP8 uncovered here may suggest that the proteins are able to fully substitute for each other. Therefore we compared their expression patterns. According to publically available microarray data, *AtGRP7* and *AtGRP8* are expressed at a similar level across plant tissues except for a lower *AtGRP8* abundance in siliques and later stages of seed development (Figure S2) (28). Moreover, the circadian maximum of *AtGRP8* transcript oscillation is only slightly advanced relative to the *AtGRP7* peak (29). Both *AtGRP7* and *AtGRP8* transcripts have been described as being upregulated by cold (11,30). We investigated steady-state protein levels under these conditions using specific anti-peptide antibodies. Two-week-old Col plants were transferred to 4°C at light onset and harvested without cold treatment and after 1, 2, 4 and 7 days, respectively. *At*GRP8 protein abundance rose marginally at best after transfer to 4°C, whereas *At*GRP7 protein abundance steadily increased up to day 7 (Figure 5A, B). The *AtGRP8* transcript level was only weakly increased at the circadian minimum (zt2) after 1 day of cold treatment but declined afterwards (Figure 5C). Also at the circadian maximum (zt10), *AtGRP8* transcript levels declined during extended exposure to cold. In contrast, a strong increase of the *AtGRP7* transcript level was observed at the circadian minimum (zt2). At the circadian maximum (zt10), the level in plants transferred to 4°C was not elevated beyond that of control plants. These data indicate that *At*GRP7 and *At*GRP8 differ in their response to cold
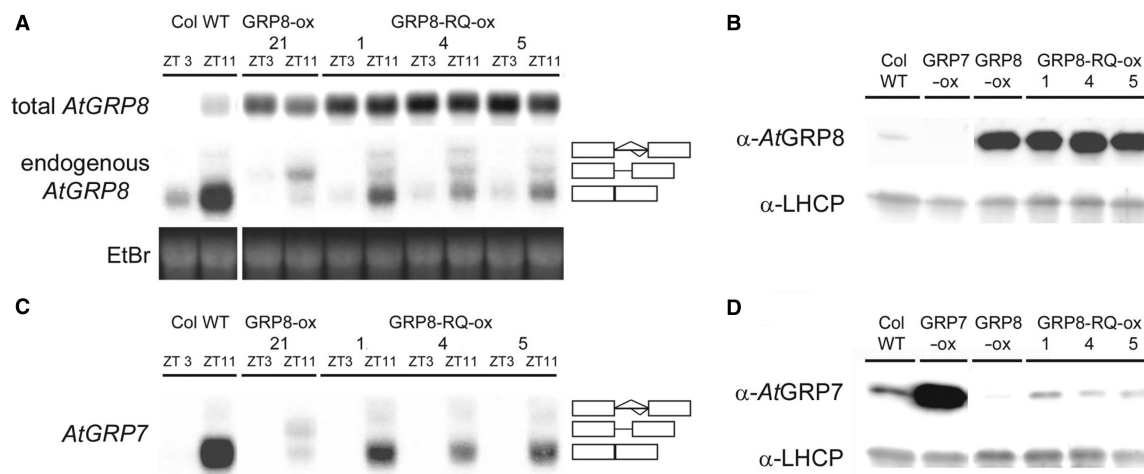
Figure 4. Molecular characterization of transgenic *At*GRP8-RQ ox lines. (**A**) WT, *At*GRP8-ox and *At*GRP8-RQ-ox plants were harvested at zt3 and zt11. The RNA gel blot was hybridized with the *AtGRP8* cDNA to determine the total transcript level (top) and with the gene-specific probe to monitor the endogenous *AtGRP8* transcript (middle). The position of the pre-mRNA, as_*AtGRP8* retaining the first half of the intron and the mRNA are indicated. Boxes represent exons, lines represent the first and the second half of the intron, respectively. The ethidium-bromide stained gel shows equal loading (bottom). (**B**) The immunoblot with total protein of WT plants, the *At*GRP8-ox lines 5 and 21, and the *At*GRP8-RQ-ox lines 1, 4 and 5, harvested at zt11, was probed with the *At*GRP8 antibody (top) and an antibody against LHCP as loading control (bottom). (**C**) The RNA gel blot shown in (A) was stripped and rehybridized with the *At*GRP7 probe. (**D**) The immunoblot with the same protein extracts as shown in (B) was probed with the *At*GRP7 antibody (top) and the LHCP antibody (bottom).

and thus do not act entirely redundant, as their expression pattern is not fully congruent.

To determine whether the exposure to low temperatures may influence the alternative splicing, the pattern of the alternative splice forms and mature mRNAs in 2-week-old plants exposed to cold for 1, 2 or 5 days was compared to that in untreated plants (Figure S3). as_*AtGRP7* accumulated in parallel with the RNA. While the *AtGRP8* mRNA only weakly and transiently increased, a stronger upregulation was observed for as_*AtGRP8*. Thus, only for *AtGRP8* a slight change in the ratio of the alternative splice forms is observed in the cold. Previous studies have demonstrated changes in the alternative splicing pattern of Arabidopsis SR genes upon cold treatment which may give rise to proteins with different domains and, consequently, changes in splicing of downstream targets (31,32).

as_*AtGRP8* and as_*AtGRP7* are direct targets of the NMD pathway

Degradation of as_*AtGRP8* and as_*AtGRP7* is dependent on AtUPF1 and AtUPF3, key components of the NMD pathway of mRNA surveillance that ensures clearance of PTC-containing mRNAs from the cellular transcriptome (12). Recently, NMD has emerged as a widespread regulatory mechanism of physiological gene expression (33–35). In the Arabidopsis *lba* (*low β-amylase*) mutant which has a point mutation in the *UPF1* gene a suite of transcripts show higher steady-state abundance, as expected for NMD substrates (36). But additionally several transcripts are down-regulated with a high proportion of sugar-inducible mRNAs, implicating AtUPF1 in sugar signalling (36).

By analogy, the elevated as_*AtGRP8* and as_*AtGRP7* levels in *upf1* and *upf3* mutants (12) may be an indirect

consequence of the reduced AtUPF1 or AtUPF3 levels. To distinguish such an indirect effect of AtUPF1 and AtUPF3 on transcription from a direct effect on transcript abundance, we assayed the pre-mRNA levels by RT–PCR. *AtGRP8* pre-mRNA steady-state abundance was not changed in the *upf1* and *upf3* mutants (Figure 6A) and also the *AtGRP7* pre-mRNA level was indistinguishable from WT (Figure 6B) in contrast to the strongly elevated as_*AtGRP7* and as_*AtGRP8* levels found in *upf1-5*, *upf3-1* and *upf3-2* (12). This indicates that the AtUPF1- and AtUPF3-dependent reduction of as_*AtGRP8* and as_*AtGRP7* is due to post-transcriptional destabilization rather than an indirect consequence of transcriptional inhibition. In higher plants, an increasing number of PTC-containing transcripts have been found to be stabilized when UPF1 and/or UPF3 functions are impaired (36–39). It has not been investigated whether some of them may be influenced either through an NMD-independent function of AtUPF1 and AtUPF3 or as a consequence of a cognate transcription factor undergoing NMD. In humans, in a survey of potential NMD targets more than 5% of the genes detected on Affymetrix GeneChips were affected by the presence or absence of UPF1 (40). For 15 out of 16 selected transcripts the pre-mRNA level was also changed, however, suggesting that the vast majority of those transcripts are affected indirectly through altered transcription rather than being *bona fide* NMD targets (40).

If the unproductive *AtGRP8* and *AtGRP7* splicing elicited by elevated levels of *At*GRP7 and *At*GRP8 protein indeed is functionally relevant, this may be reflected at the level of sequence conservation. The gene structure of the small glycine-rich RNA-binding proteins with a single RRM is well conserved among different plant species, harboring a single intron of similar size between RNP2 and RNP1, and a predicted cryptic 5′ splice site (8,19).
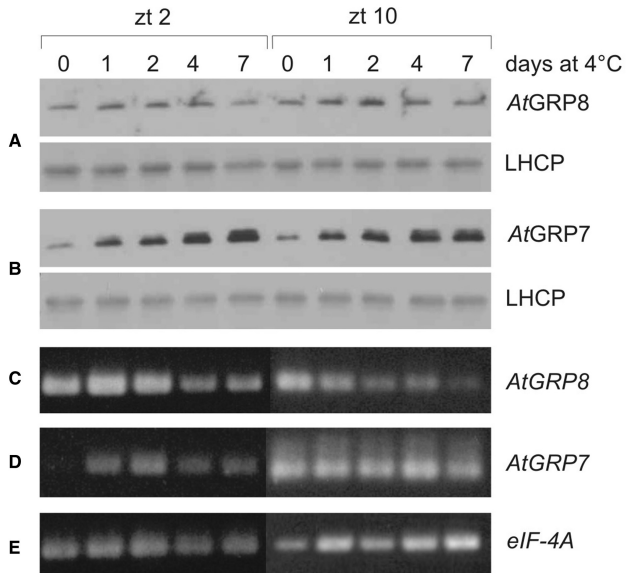
Figure 5. Differential regulation by cold of *AtGRP8* and *AtGRP7*. (**A**) Col plants grown for 2 weeks in 16 h light/8 h dark cycles at 20°C were transferred to 16-h light/8-h dark cycles at 4°C and harvested on day 0, 1, 2, 4 and 7 at zt2 and zt10, respectively. (**B**) Immunoblots with total protein extracts from the same plants were probed with the *At*GRP8 (A, top) and *At*GRP7 (B, top) antibodies and an LHCP antibody (A and B, bottom) as loading control. (**C**) Semiquantitative RT-PCR of *AtGRP8*. (**D**) Semiquantitative RT-PCR of *AtGRP7*. (**E**) Semiquantitative RT-PCR of *eIF-4A* as constitutive control. The exponential range was determined by comparing the signal with increasing number of cycles. The absence of genomic DNA was confirmed with nonretrotranscribed RNA.

Notably, the retained upstream part of the intron exhibits a higher degree of conservation than the downstream part spliced out in the as_*AtGRP7* and as_*AtGRP8* variants (Figure 7). A comparison of *AtGRP8* with *AtGRP7* and orthologs from mustard, oilseed rape, tobacco and Pelargonium shows that the degree of conservation reaches that of the surrounding exons (Figure 7, Table S1). The open reading frames contain an *in frame* termination codon within the first half of the intron and code for predicted 5 kDa polypeptides comprising only the RNP2 moiety of the RRM. As intact RNP1 is important for high-affinity RNA binding of *At*GRP7 (12) and *At*GRP8 (Table 2), these truncated polypeptides presumably do not interact with the RNA target sites in a productive manner but theoretically, they could interfere with *At*GRP7 and *At*GRP8 function. So far, however, these polypeptides have not been detected in Arabidopsis WT plants, the *upf* mutants or in *Sinapis alba* (data not shown). Thus, the conservation likely is not due to protein coding and therefore implies a regulatory function, e.g. to convey degradation when retained.

A similar scenario has been observed for the ribosomal protein L12 in *Caenorhabditis elegans* (41). Elevated L12 levels promote the formation of an alternatively spliced transcript with a PTC due to removal of a partial intron. Thus, this autoregulatory circuit also couples unproductive splicing with destruction via the NMD pathway and, like for *AtGRP7* and *AtGRP8*, the retained part
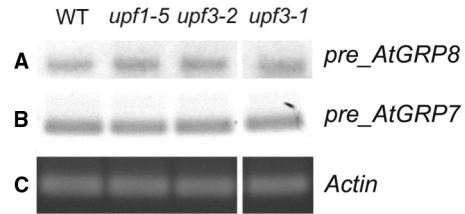

Figure 6. Effect of *upf1* and *upf3* mutations on steady-state abundance of the *AtGRP8 and AtGRP7* pre-mRNAs. RNA from the *upf1-5*, *upf3-1* and *upf3-2* mutants and WT harvested at zt10 was reverse-transcribed. PCR amplification of the *AtGRP8* (**A**) and *AtGRP7* pre-mRNA (**B**) was performed using specific primers and 24 cycles. The gel with the PCR products was blotted and hybridized with the *AtGRP8* cDNA (**A**) or *AtGRP7* cDNA (**B**). Amplification with *ACTIN* primers served as control (**C**).

of the intron displays a striking sequence conservation in worms (41).

Notably, the *AtGRP7* transcript oscillates with one of the highest amplitudes observed for circadian genes in Arabidopsis (19). Following transcriptional activation by the circadian clock during the day and a steep rise in mRNA level, the *AtGRP7* mRNA needs to decay during the declining phase below a level attained by time-of-day dependent transcriptional control alone in order to prevent damping (19,35). One way to accomplish high-amplitude mRNA oscillations would be by severely decreasing mRNA half life during the course of the day (42). However, such a scenario would also impact non-clock functions of *At*GRP7 and *At*GRP8, as in addition to their regulation by the circadian clock *AtGRP8* and in particular *AtGRP7* respond to numerous external factors (28). Transcriptional activation by external regulatory cues presumably would not bring about sufficiently high levels of a short-lived mRNA during a considerable part of the day to allow increase in protein steady-state abundance. Thus, AS-NMD elicited by the proteins themselves may be an efficient way to adjust mRNA and consequently protein levels.

Utilization of NMD for negative autoregulation has been widely observed for proteins involved in splicing regulation. The mammalian SR protein SC35 downregulates its expression through alternative splicing, resulting in an unstable transcript (43). However, in contrast to as_*At*GRP7 and as_*At*GRP8, the alternative SC35 transcripts retain full coding capacity. Crossregulation recently has been described for the polypyrimidine tract-binding protein (PTB), a global repressor of alternative splicing in nonneuronal cells, and its neurally expressed paralogue nPTB. PTB induces skipping of its own exon 11, producing an NMD substrate, and also induces exon-skipping in nPTB, resulting in a switch from PTB to nPTB expression during the development of neurons that impacts neural-specific splicing patterns of downstream targets. nPTB is able to autoregulate at the level of exon skipping when PTB is absent (44). Spellman showed that nPTB is able to repress PTB exon 11, however whether this occurs *in vivo* has not yet been determined (45).

For *AtGRP7* and *AtGRP8* we have found autoregulation and reciprocal crossregulation, showing that the

newly identified *At*GRP8 feedback loop is interconnected with the *At*GRP7 feedback loop previously identified as a circadian slave oscillator (9). The connection between the two regulatory circuits may serve to integrate input by diverse stimuli, and the crossregulation may fine tune and balance the expression of both proteins.

In the future it will be important to determine common target transcripts of *At*GRP7 and *At*GRP8 and to determine the relative influence both proteins have on such downstream transcripts.

CONCLUSION

We show here that the clock-controlled RNA-binding protein *At*GRP8 forms an interlocked post-transcriptional negative feedback loop with the *At*GRP7 autoregulatory circuit. Both proteins negatively autoregulate and reciprocally crossregulate by binding to their pre-mRNAs and promoting unproductive splicing coupled to degradation via the NMD pathway (Figure 8). Thus, we extend the examples of quantitative post-transcriptional control by
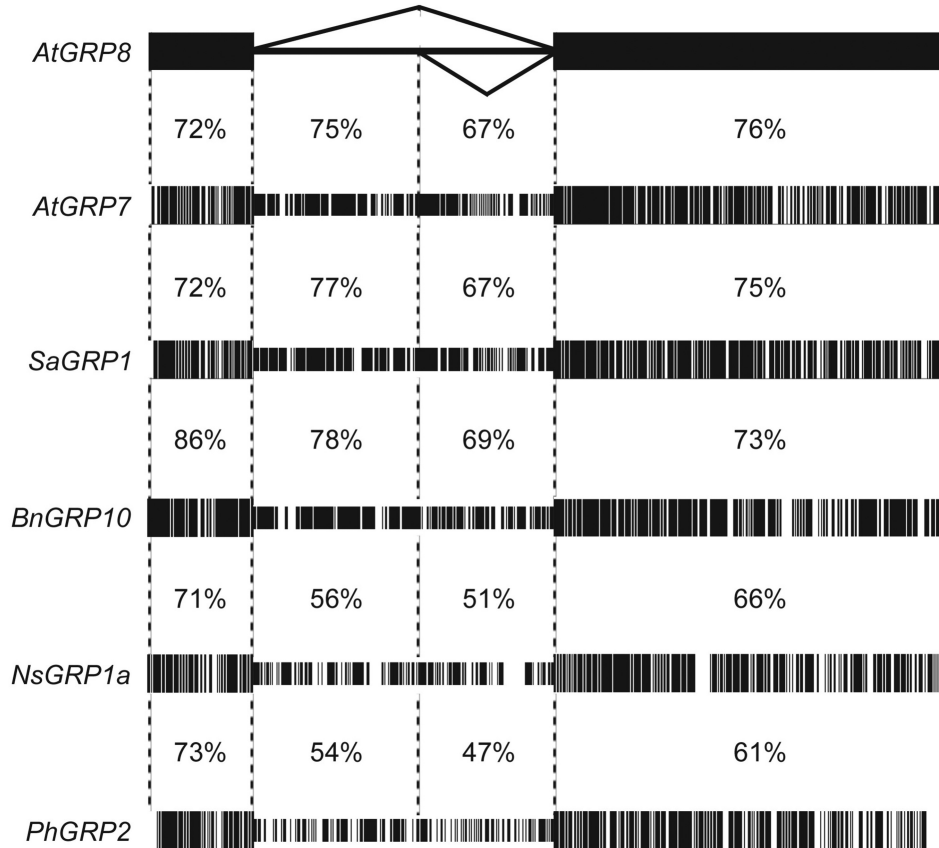

Figure 7. Conservation of the retained part of the GRP introns. The nucleotide sequence corresponding to *AtGRP8* exon I, exon II and the intron was aligned with the corresponding sequence of *AtGRP7*, *SaGRP1* (8), *BnGRP10* (46), *NsGRP1a* (47) and *PhGRP2* (48).
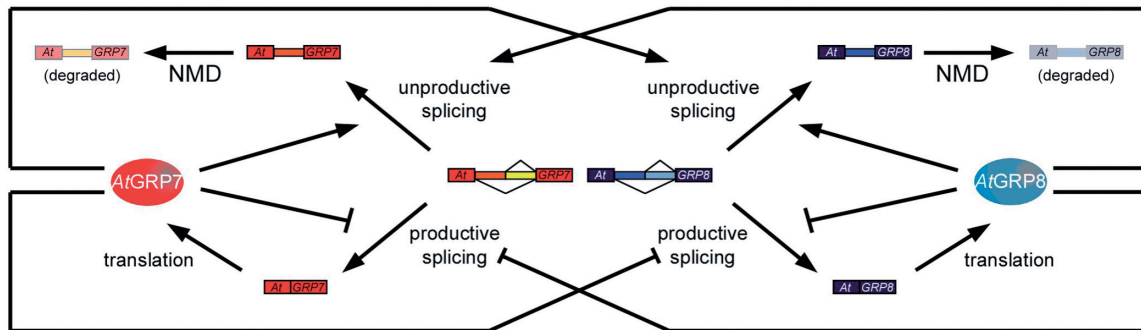

Figure 8. Model of the interlocked *At*GRP7 and *At*GRP8 feedback loops. Increasing *At*GRP7 and *At*GRP8 protein (depicted as ellipses) levels promote use of the cryptic intronic 5′ splice sites, leading to unproductively spliced as_*AtGRP7* and as_*AtGRP8* transcripts that are degraded via the NMD pathway.

AS-NMD to autoregulatory loops in output pathways of the circadian clock.

SUPPLEMENTARY DATA

Supplementary Data are available at NAR Online.

ACKNOWLEDGEMENTS

FUNDING

REFERENCES

1. Cheng,Y. and Chen,X. (2004) Posttranscriptional control of plant development. *Curr. Opin. Plant Biol.*, **7**, 20–25.
2. Staiger,D. (2001) RNA-binding proteins and circadian rhythms in *Arabidopsis thaliana*. *Philos. Trans. R. Soc. Lond. B. Biol. Sci.*, **356**, 1755–1759.
3. Reddy,A.S. (2007) Alternative splicing of pre-messenger RNAs in plants in the genomic era. *Annu. Rev. Plant Biol.*, **58**, 267–294.
4. Lorkovic,Z.J., Wieczorek Kirk,D.A., Lambermon,M.H. and Filipowicz,W. (2000) Pre-mRNA splicing in higher plants. *Trends Plant Sci.*, **5**, 160–167.
5. Lorkovic,Z.J. and Barta,A. (2002) Genome analysis: RNA recognition motif (RRM) and K homology (KH) domain RNA-binding proteins from the flowering plant *Arabidopsis thaliana*. *Nucleic Acids Res.*, **30**, 623–635.
6. Maris,C., Dominguez,C. and Allain,F.H. (2005) The RNA recognition motif, a plastic RNA-binding platform to regulate post-transcriptional gene expression. *FEBS J.*, **272**, 2118–2131.
7. van Nocker,S. and Vierstra,R.D. (1993) Two cDNAs from Arabidopsis thaliana encode putative RNA binding proteins containing glycine-rich domains. *Plant Mol. Biol.*, **21**, 695–699.
8. Heintzen,C., Melzer,S., Fischer,R., Kappeler,S., Apel,K. and Staiger,D. (1994) A light- and temperature-entrained circadian clock controls expression of transcripts encoding nuclear proteins with homology to RNA-binding proteins in meristematic tissue. *Plant J.*, **5**, 799–813.
9. Heintzen,C., Nater,M., Apel,K. and Staiger,D. (1997) *At*GRP7, a nuclear RNA-binding protein as a component of a circadian-regulated negative feedback loop in *Arabidopsis thaliana*. *Proc. Natl Acad. Sci. USA*, **94**, 8515–8520.
10. Fu,Z.Q., Guo,M., Jeong,B.R., Tian,F., Elthon,T.E., Cerny,R.L., Staiger,D. and Alfano,J.R. (2007) A type III effector ADP-ribosylates RNA-binding proteins and quells plant immunity. *Nature*, **447**, 284–288.
11. Carpenter,C.D., Kreps,J.A. and Simon,A.E. (1994) Genes encoding glycine-rich *Arabidopsis thaliana* proteins with RNA-binding motifs are influenced by cold treatment and an endogenous circadian rhythm. *Plant Physiol.*, **104**, 1015–1025.
12. Schöning,J.C., Streitner,C., Page,D.R., Hennig,S., Uchida,K., Wolf,E., Furuya,M. and Staiger,D. (2007) Autoregulation of the circadian slave oscillator component *At*GRP7 and regulation of its

13. targets is impaired by a single RNA recognition motif point mutation. *Plant J.*, **52**, 1119–1130.
13. Staiger,D., Zecca,L., Wieczorek Kirk,D.A., Apel,K. and Eckstein,L. (2003) The circadian clock regulated RNA-binding protein AtGRP7 autoregulates its expression by influencing alternative splicing of its own pre-mRNA. *Plant J.*, **33**, 361–371.
14. Rudolf,F., Wehrle,F. and Staiger,D. (2004) Slave to the rhythm. *The Biochemist*, **26**, 11–13.
15. Streitner,C., Danisman,S., Wehrle,F., Schöning,J.C., Alfano,J.R. and Staiger,D. (2008) The small glycine-rich RNA-binding protein AtGRP7 promotes floral transition in *Arabidopsis thaliana*. *Plant J.*, **56**, 239–250.
16. Becker,D., Kemper,E., Schell,J. and Masterson,R. (1992) New plant binary vectors with selectable markers located proximal to the left T-DNA border. *Plant Mol. Biol.*, **20**, 1195–1197.
17. Bechthold,N., Ellis,J. and Pelletier,G. (1993) In planta *Agrobacterium*-mediated gene transfer by infiltration of adult *Arabidopsis thaliana* plants. *Science de la vie/Life Sci.*, **316**, 1194–1199.
18. Murashige,T. and Skoog,F. (1962) A revised medium for rapid growth and bio assays with tobacco tissue cultures. *Physiol. Plant.*, **15**, 473–497.
19. Staiger,D. and Apel,K. (1999) Circadian clock-regulated expression of an RNA-binding protein in Arabidopsis: characterisation of a minimal promoter element. *Mol. Gen. Genet*, **261**, 811–819.
20. Pedersen,J.S., Meyer,I.M., Forsberg,R., Simmonds,P. and Hein,J. (2004) A comparative method for finding and folding RNA secondary structures within protein-coding regions. *Nucleic Acids Res.*, **32**, 4925–4936.
21. Pedersen,J.S., Forsberg,R., Meyer,I.M. and Hein,J. (2004) An evolutionary model for protein-coding regions with conserved RNA structure. *Mol. Biol. Evol.*, **21**, 1913–1922.
22. Thompson,J.D., Higgins,D.G. and Gibson,T.J. (1994) CLUSTAL W: improving the sensitivity of progressive multiple sequence alignment through sequence weighting, position-specific gap penalties and weight matrix choice. *Nucleic Acids Res.*, **22**, 4673–4680.
23. Kalyna,M., Lopato,S. and Barta,A. (2003) Ectopic expression of atRSZ33 reveals its function in splicing and causes pleiotropic changes in development. *Mol. Biol. Cell*, **14**, 3565–3577.
24. Kalyna,M., Lopato,S., Voronin,V. and Barta,A. (2006) Evolutionary conservation and regulation of particular alternative splicing events in plant SR proteins. *Nucleic Acids Res.*, **34**, 4395–4405.
25. Ding,J., Hayashi,M.K., Zhang,Y., Manche,L., Krainer,A.R. and Xu,R.M. (1999) Crystal structure of the two-RRM domain of hnRNP A1 (UP1) complexed with single-stranded telomeric DNA. *Genes Dev.*, **13**, 1102–1115.
26. Jessen,T.H., Oubridge,C., Teo,C.-H., Pritchard,C. and Nagai,K. (1991) Identification of molecular contacts between the U1 A small nuclear ribonucleoprotein and U1 RNA. *EMBO J.*, **10**, 3447–3456.
27. Nagai,K., Oubridge,C., Jessen,T.H., Li,J. and Evans,P.R. (1990) Crystal structure of the RNA-binding domain of the U1 small nuclear ribonucleoprotein A. *Nature*, **348**, 515–520.
28. Zimmermann,P., Hirsch-Hoffmann,M., Hennig,L. and Gruissem,W. (2004) GENEVESTIGATOR. Arabidopsis Microarray Database and Analysis Toolbox. *Plant Physiol.*, **136**, 2621–6232.
29. Harmer,S.L., Hogenesch,J.B., Straume,M., Chang,H.S., Han,B., Zhu,T., Wang,X., Kreps,J.A. and Kay,S.A. (2000) Orchestrated transcription of key pathways in Arabidopsis by the circadian clock. *Science*, **290**, 2110–2113.
30. Kwak,K.J., Kim,Y.O. and Kang,H. (2005) Characterization of transgenic Arabidopsis plants overexpressing GR-RBP4 under high salinity, dehydration, or cold stress. *J. Exp. Bot.*, **56**, 3007–3016.
31. Lazar,G. and Goodman,H. (2000) The *Arabidopsis* splicing factor SR1 is regulated by alternative splicing. *Plant Mol. Biol.*, 571–581.
32. Palusa,S.G., Ali,G.S. and Reddy,A.S. (2007) Alternative splicing of pre-mRNAs of Arabidopsis serine/arginine-rich proteins: regulation by hormones and stresses. *Plant J.*, **49**, 1091–1107.
33. Rehwinkel,J., Raes,J. and Izaurralde,E. (2006) Nonsense-mediated mRNA decay: Target genes and functional diversification of effectors. *Trends Biochem. Sci.*, **31**, 639–646.
34. Guan,Q., Zheng,W., Tang,S., Liu,X., Zinkel,R.A., Tsui,K.W., Yandell,B.S. and Culbertson,M.R. (2006) Impact of nonsense-

mediated mRNA decay on the global expression profile of budding yeast. *PLoS Genet.*, **2**, e203.

35. McGlincy,N.J. and Smith,C.W. (2008) Alternative splicing resulting in nonsense-mediated mRNA decay: what is the meaning of nonsense? *Trends Biochem. Sci.*, **33**, 385–393.

36. Yoine,M., Ohto,M.A., Onai,K., Mita,S. and Nakamura,K. (2006) The lba1 mutation of UPF1 RNA helicase involved in nonsense-mediated mRNA decay causes pleiotropic phenotypic changes and altered sugar signalling in Arabidopsis. *Plant J.*, **47**, 49–62.

37. Hori,K. and Watanabe,Y. (2005) UPF3 suppresses aberrant spliced mRNA in *Arabidopsis. Plant J.*, **43**, 530–540.

38. Arciga-Reyes,L., Wootton,L., Kieffer,M. and Davies,B. (2006) UPF1 is required for nonsense-mediated mRNA decay (NMD) and RNAi in Arabidopsis. *Plant J.*, **47**, 480–489.

39. Wu,J., Kang,J.-H., Hettenhausen,C. and Baldwin,I.T. (2007) Nonsense-mediated mRNA decay (NMD) silences the accumulation of aberrant trypsin proteinase inhibitor mRNA in Nicotiana attenuata. *Plant J.*, **51**, 693–706.

40. Viegas,M.H., Gehring,N.H., Breit,S., Hentze,M.W. and Kulozik,A.E. (2007) The abundance of RNPS1, a protein component of the exon junction complex, can determine the variability in efficiency of the Nonsense Mediated Decay pathway. *Nucleic Acids Res.*, **35**, 4542–4551.

41. Mitrovich,Q.M. and Anderson,P. (2000) Unproductively spliced ribosomal protein mRNAs are natural targets of mRNA surveillance in C. elegans. *Genes Dev.*, **14**, 2173–2184.

42. So,W.V. and Rosbash,M. (1997) Post-transcriptional regulation contributes to Drosophila clock gene mRNA cycling. *EMBO J.*, **16**, 7146–7155.

43. Sureau,A., Gattoni,R., Dooghe,Y., Stevenin,J. and Soret,J. (2001) SC35 autoregulates its expression by promoting splicing events that destabilize its mRNAs. *EMBO J.*, **20**, 1785–1796.

44. Boutz,P.L., Stoilov,P., Li,Q., Lin,C.H., Chawla,G., Ostrow,K., Shiue,L., Ares,M. Jr. and Black,D.L. (2007) A post-transcriptional regulatory switch in polypyrimidine tract-binding proteins reprograms alternative splicing in developing neurons. *Genes Dev.*, **21**, 1636–1652.

45. Spellman,R., Llorian,M. and Smith,C.W. (2007) Crossregulation and functional redundancy between the splicing regulator PTB and its paralogs nPTB and ROD1. *Mol. Cell*, **27**, 420–434.

46. Bergeron,D., Beauseigle,D. and Bellemare,G. (1993) Sequence and expression of a gene encoding a protein with RNA-binding and glycine-rich domains in *Brassica napus. Biochim. Biophys. Acta*, **1216**, 123–125.

47. Hirose,T., Sugita,M. and Sugiura,M. (1993) cDNA structure, expression and nucleic acid-binding properties of three RNA-binding proteins in tobacco: occurrence of tissue-specific alternative splicing. *Nucleic Acids Res.*, **21**, 3981–3987.

48. Clark,D.G., Richards,C. and Brown,K.M. (1999) Characterization of circadian-regulated mRNAs encoding glycine-rich RNA-binding proteins in Pelargonium hortorum. *Physiol. Plant.*, **106**, 409–414.